Electronic Supplementary Information

Electrocatalytic hydrogen evolution with a copper porphyrin bearing *meso*-(*o*-carborane) substituents

Xinyang Peng, Jinxiu Han, Xialiang Li, Guijun Liu, Yuhan Xu, Yuxin Peng, Shuai Nie, Wenzi Li, Xinrui Li, Zhuo Chen, Haonan Peng,* Rui Cao* and Yu Fang.

Key Laboratory of Applied Surface and Colloid Chemistry, Ministry of Education, School of Chemistry and Chemical Engineering, Shaanxi Normal University, Xi'an 710119, China.

Correspondence E-mail: phn@snnu.edu.cn, ruicao@snnu.edu.cn

General Materials and Methods.

Manipulations of air- and moisture-sensitive materials were performed under nitrogen gas using standard Schlenk line techniques. All reagents used in this work were purchased from commercial suppliers and were used directly without further purification unless otherwise stated. All solvents used in this work were reagent grades. Dry solvents, including dichloromethane, tetrahydrofuran, acetonitrile, chloroform and methanol were purified by passage through activated alumina. Toluene was refluxed over sodium blocks and distilled under reduced pressure. All aqueous solutions were prepared freshly using Milli-Q water.

High-resolution mass spectra (HRMS) were acquired using a Brüker MAXIS apparatus. ^{1}H NMR spectra were acquired using JEOL spectrometer operating at 400 MHz. UV-vis spectra were collected on a Hitachi U-3310 Spectrophotometer. Hitachi SU8020 cold-emission field emission scanning electron microscope (FE-SEM) with an accelerating voltage of 1 kV was used to study the sample morphology. JEOL JEM-2100 with a 200 kV accelerating voltage was used to acquire transmission electron microscopy (TEM) images. X-ray photoelectron spectroscopy (XPS) was performed by using a Kratos AXIS ULTRA using monochromatic Al Kα X-ray ($h\nu$ = 1486.6 eV) with a photoelectron take-off angle of 90° with respect to the surface plane.

Electrochemical Studies.

Electrochemical studies in organic solutions. All electrochemical measurements in this work were tested using a CH instruments (model CHI660E

Electrochemical Analyzer). The cyclic voltammograms (CVs) were recorded in acetonitrile containing 0.10 M Bu_4NPF_6 and 0.50 mM catalyst at 20 °C using a three-compartment cell, which included glassy carbon as the working electrode, graphite electrode as the auxiliary electrode, and $Ag/AgNO_3$ (BASi, 10 mM $AgNO_3$, 0.10 M Bu_4NPF_6 in acetonitrile) as the reference electrode. The tests were performed after bubbling the solution with N_2 for 30 min. The glassy carbon electrode was used after polishing with α-Al_2O_3 of decreasing size (1.0 μm to 50 nm) and washing with distilled water and acetonitrile. Ferrocene was added as an internal standard. The electrolysis in acetonitrile was performed in a three-compartment electrochemical cell using a glassy carbon plate working electrode (1.0 cm^2). The H_2 detection was carried out using an SP-6890 gas chromatograph.

Electrochemical studies in aqueous solutions. The linear sweep voltammograms (LSVs) were acquired in 0.50 M H_2SO_4 using a three-compartment cell with a glassy carbon working electrode, a graphite rod auxiliary electrode, and a Ag/AgCl (saturated with KCl) reference electrode. The preparation of catalyst-coated glassy carbon electrode is described as follows. To 1.0 mL freshly distilled acetonitrile, were added 1.0 mg CNTs, 1.0 mg catalysts, and 25 μL Nafion (5.0 wt%, DuPont). The resulted mixture was sonicated using an ultrasonic cleaner for 30 min to get an ink. Then, 4 μL of the suspension was dropped onto the surface of a freshly polished glassy carbon electrode. After drying at room temperature, the prepared glassy carbon electrodes were used for electrochemical studies. The aqueous 0.50 M H_2SO_4 solution

was bubbled with N_2 for 30 min before analysis. The electrolysis of **1**/CNT and **2**/CNT was performed with a three electrode H-type cell containing a Nafion membrane (Nafion®117, DuPont, Inc.) to separate the carbon paper (0.5 cm^2, loading with catalysts) working electrode and the other two electrodes. The Faradaic efficiency (FE) tests were carried out according to the method we reported previously.[1]

X-ray Diffraction Studies.

Crystals of high quality were obtained by slow evaporation of the hexane and dichloromethane solution of Cu porphyrins at room temperature under dark. The complete data sets of **1** (CCDC 2269772), **2** (CCDC 2271198) and **c** (CCDC 2271197) were collected. The crystals suitable for X-ray diffraction studies were each suspended on a small fiber loop coating with Paratone-N oil, and cooled under a gas stream at 153(2) K on a Bruker D8 Venture X-ray diffractometer. Diffraction intensities were measured using graphite-monochromated Mo Kα radiation (λ = 0.71073 Å). Data collection, indexing, data reduction and final unit cell refinements were carried out using APEX2.[2] Absorption corrections were applied using the program SADABS.[3] The structures were solved with direct methods using SHELXS[4] and refined against F^2 on all data by full-matrix least squares with SHELXL-97,[5] following established refinement strategies. Details of the data quality and a summary of the residual values of the refinements are listed in Table S1. The three X-ray structures were checked using IUCr's CheckCIF routine, which resulted in no level A and B alerts.

Synthesis of Cu porphyrin 1.

The synthetic route of **1** is depicted in Scheme S1.

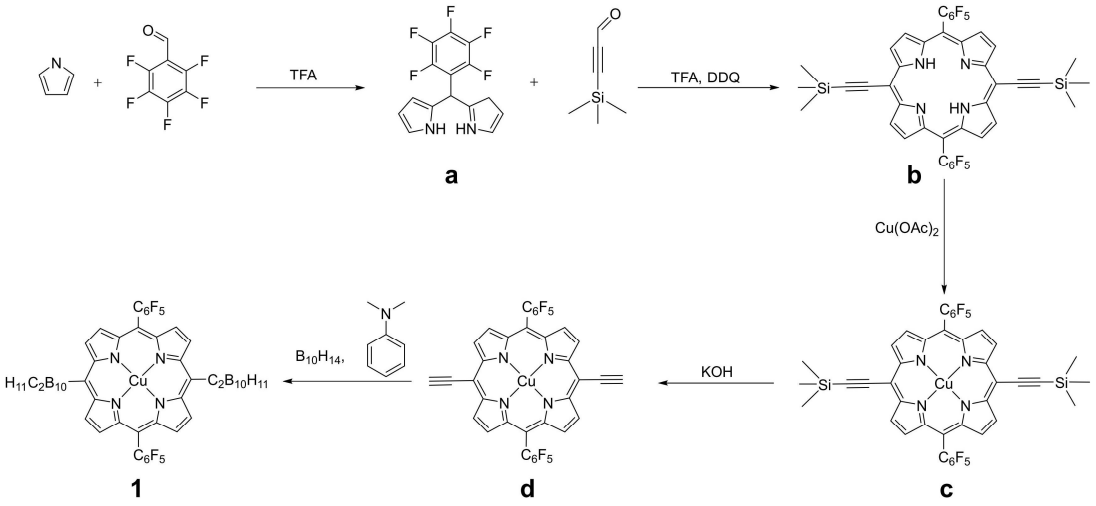

Scheme S1 Synthetic route of **1**.

Synthesis of a. To a 100 mL flask equipped with a magnetic stirring bar, were added pyrrole (45.0 mL, 650 mmol) and pentafluorobenzaldehyde (4.90 g, 25.0 mmol). After 5 min of stirring, 186 μL (2.50 mmol) trifluoroacetic acid (TFA) was dropped into the flask. The solution was stirred for 10 min at room temperature. After that, a solution of 1.0 M KOH was added to neutralize the excess TFA. The resulted solution was extracted three times using ethyl acetate and was washed with water. The organic phases were collected and were dried over Na_2SO_4. The crude products were purified by silica chromatography (hexane:dichloromethane = 5:1, v/v) to afford 7.04 g (22.5 mmol, 90.3% yield) dark yellow solids of **a**. ^{1}H NMR (400 MHz, $CDCl_3$): δ = 8.10 (s, 2H), 6.73 (m, 2H), 6.18 (q, *J* = 2.8 Hz, 2H), 6.03 (s, 2H), 5.90 (s, 1H) (Fig. S1).

Synthesis of b. To a 500 mL flask equipped with a magnetic stirring bar, were added 1.00 g **a** (3.23 mmol), 300 mL distilled dichloromethane and 475 μL 3-trimethylsilylpropynal (3.20 mmol). After bubbling with N_2 for 30 min, 240 μL TFA (3.23 mmol) was dropped slowly to the solution under dark. With 30 min stirring under N_2, 733 mg 2,3-dichloro-5,6-dicyano-1,4-benzoquinone (DDQ, 3.23 mmol) was added into the solution. After another 5 min reaction, the solution was filtered by a crude silica chromatography. The solution with red fluorescence was collected and the solvent was removed by a rotary evaporator. The crude products were purified by another silica chromatography (hexane:dichloromethane = 50:1, v/v) to afford 150 mg (0.180 mmol, 11.1% yield) purple solids of **b**. ^{1}H NMR (400 MHz, $CDCl_3$): δ = 9.68 (d, *J* = 4.8 Hz, 4H), 8.76 (d, *J* = 4.8 Hz, 4H), 0.61 (s, 18H), −2.28 (s, 2H) (Fig. S2).

Synthesis of c. To a 250 mL flask equipped with a magnetic stirring bar, were added 90.0 mL $CHCl_3$ and 80.0 mg **b** (0.096 mmol) under dark. Then, a 30.0 mL methanol solution of $Cu(OAc)_2 \cdot H_2O$ (572 mg, 2.88 mmol) was added into to the flask. After refluxing the solution for 3 h under dark, the solvent was removed by a rotary evaporator. The crude products were dissolved in dichloromethane and were washed with H_2O for three times to remove the excess copper salts. After drying with Na_2SO_4, silica chromatography (hexane:dichloromethane = 30:1, v/v) was used for purification to give 79.0 mg (0.088 mmol, 92.0% yield) dark purple solids of **c**. HRMS of $[M+H]^+$: calcd. $C_{42}H_{27}CuF_{10}N_4Si_2$, 896.0905, found, 896.0904 (Fig. S4).

Synthesis of d. To a 100 mL flask equipped with a magnetic stirring bar, were added 50.0 mL tetrahydrofuran, 50.0 mg **c** (0.056 mmol) and 31.2 mg KOH (0.56 mmol). The mixture was stirred for 1 h under dark, and the solvent was then removed with a rotary evaporator. The crude products were washed with water and filtered to remove the excess KOH. After drying at room temperature, the dark purple solids of **d** were used directly for the next reaction without further purification due to its poor solubility, HRMS of $[M+H]^+$: calcd. $C_{36}H_{11}CuF_{10}N_4$, 752.0115, found, 752.0105 (Fig. S5).

Synthesis of 1. To a 100 mL oven-dried flask equipped with a stirring bar, were added **d** from the last step and 40.8 mg decaborane ($B_{10}H_{14}$, 0.335 mmol). After purging the flask with N_2, 10.0 mL distilled toluene and 42.5 μL N,N-dimethylaniline (0.335 mmol) were added. The solution was bubbled with N_2 for 30 min, and then the temperature was raised to 110 °C for 10 h under dark. After cooling down to room temperature, the solvent was removed with a rotary evaporator to get the crude product, which was purified by silica chromatography (hexanes:dichloromethane = 20:1, v/v) to afford 8.00 mg (0.0081 mmol, 14.5% yield, calculated for the combined two steps) dark green solids of **1**. HRMS of $[M+H]^+$: calcd. for $C_{36}H_{31}B_{20}CuF_{10}N_4$, 992.3597, found, 992.3616 (Fig. S6).

Synthesis of 2.

The synthetic route of **2** is depicted in Scheme S2.

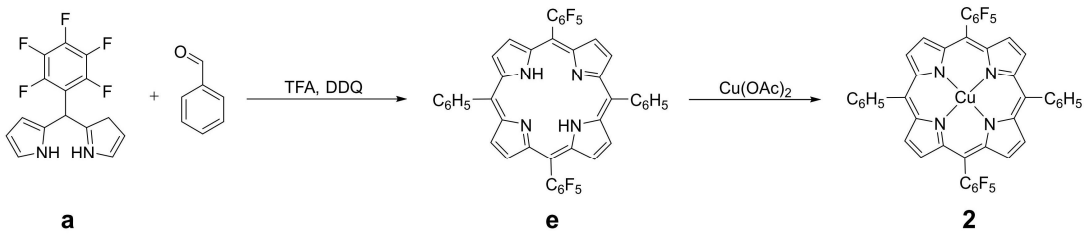

a **e** **2**

Scheme S2 Synthetic route of **2**.

Synthesis of e. To 300 mL distilled dichloromethane, were added 1.50 g (4.84 mmol) **a** and 493 μL (4.84 mmol) benzaldehyde. After bubbling the solution with N_2 for 30 min, 360 μL TFA (4.84 mmol) was slowly dropped into the solution under dark. After 1.5 h of reaction, 1.10 g DDQ (4.84 mmol) was added, and the mixture was stirred for another 20 min. Purification by silica chromatography (hexane:dichloromethane = 30:1, v/v) afforded 270 mg (0.340 mmol, 14.0% yield) dark purple solids of **e**. ^{1}H NMR (400 MHz, $CDCl_3$): δ = 8.98 (d, *J* = 4.8 Hz, 4H), 8.84 (d, *J* = 4.8 Hz, 4H), 8.25 (dd, *J* = 7.6 Hz, 1.6 Hz, 4H), 7.77- 7.85 (m, 6H), −2.82 (s, 2H) (Fig. S3).

Synthesis of 2. To a 250 mL flask equipped with a magnetic stirring bar, were added 50.0 mg (0.0630 mmol) **e**, 80.0 mL $CHCl_3$ and 376 mg (1.89 mmol) $Cu(OAc)_2 \cdot H_2O$, which was dissolved in 25 mL methanol. The mixture was refluxed overnight under dark, and the solvent was removed by a rotary evaporator. After washing with water for three times, the crude product was purified by silica chromatography (hexane:dichloromethane = 15:1, v/v) to afford 47.0 mg (0.0550 mmol, 87% yield) dark red solids of **2**. HRMS of $[M+H]^+$: calcd. for $C_{44}H_{19}CuF_{10}N_4$, 856.0741, found, 856.0742 (Fig. S7).

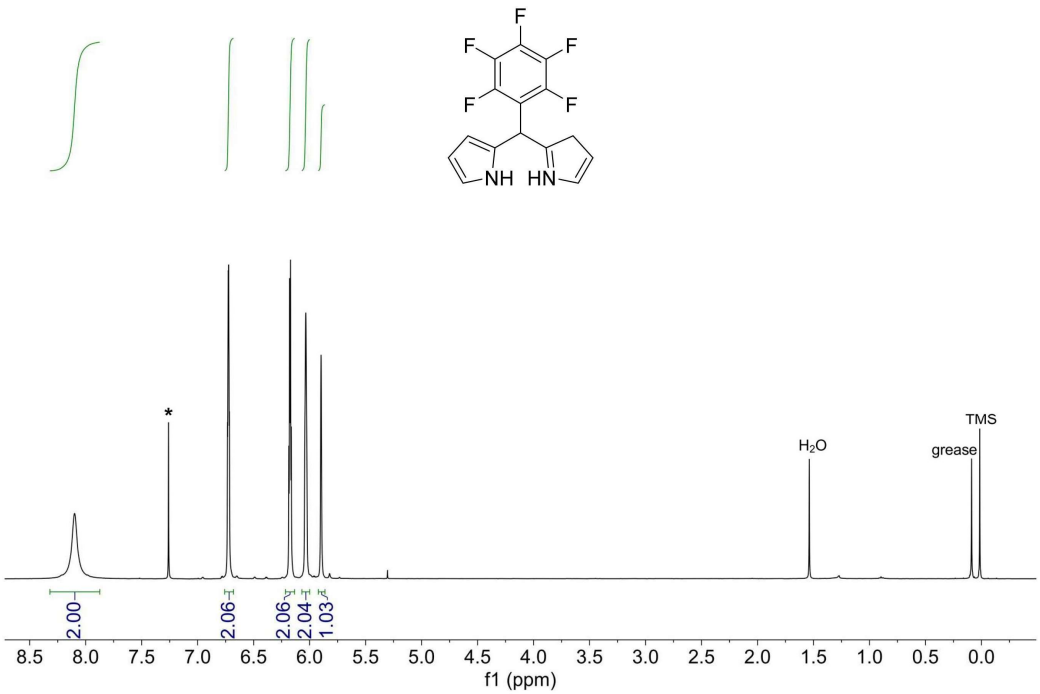

Fig. S1 ^{1}H NMR spectrum of **a** in $CDCl_3$. The solvent residue peak is labeled (*).

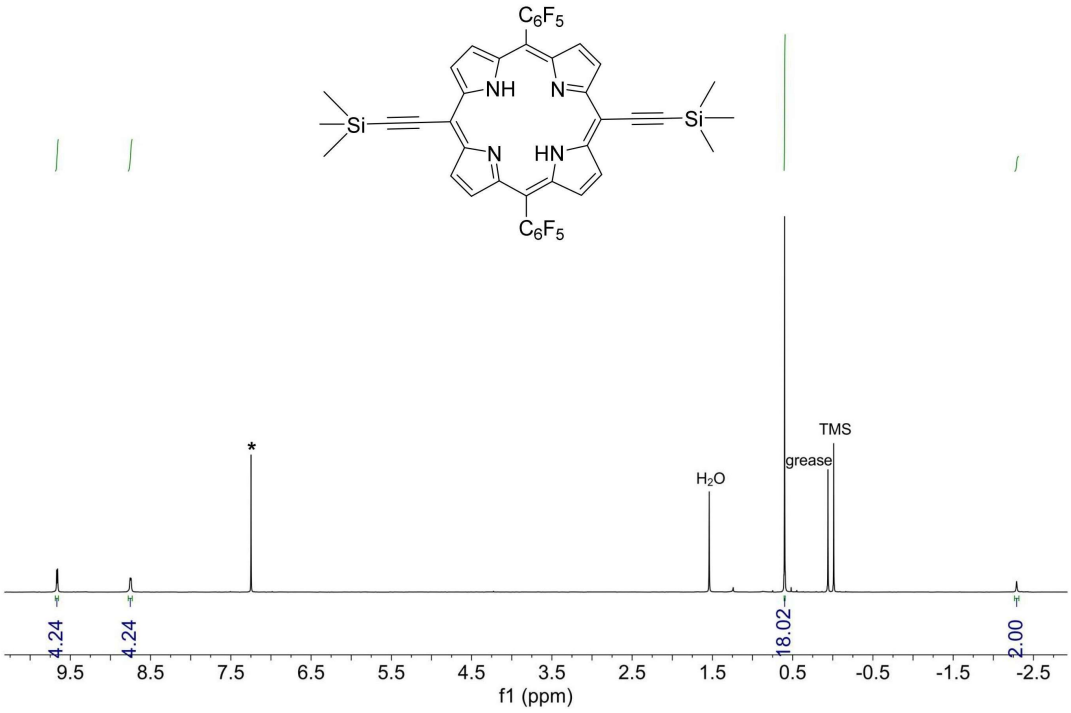

Fig. S2 ^{1}H NMR spectrum of **b** in $CDCl_3$. The solvent residue peak is labeled (*).

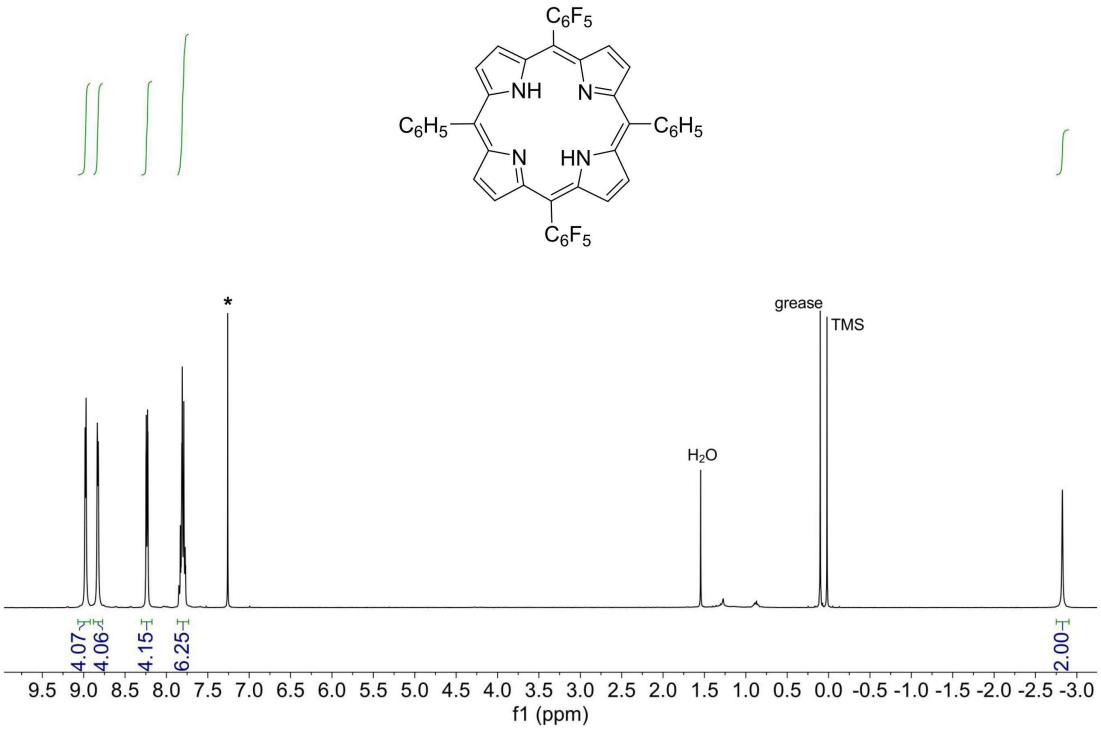

Fig. S3 ^{1}H NMR spectrum of **e** in $CDCl_3$. The solvent residue peak is labeled (*).

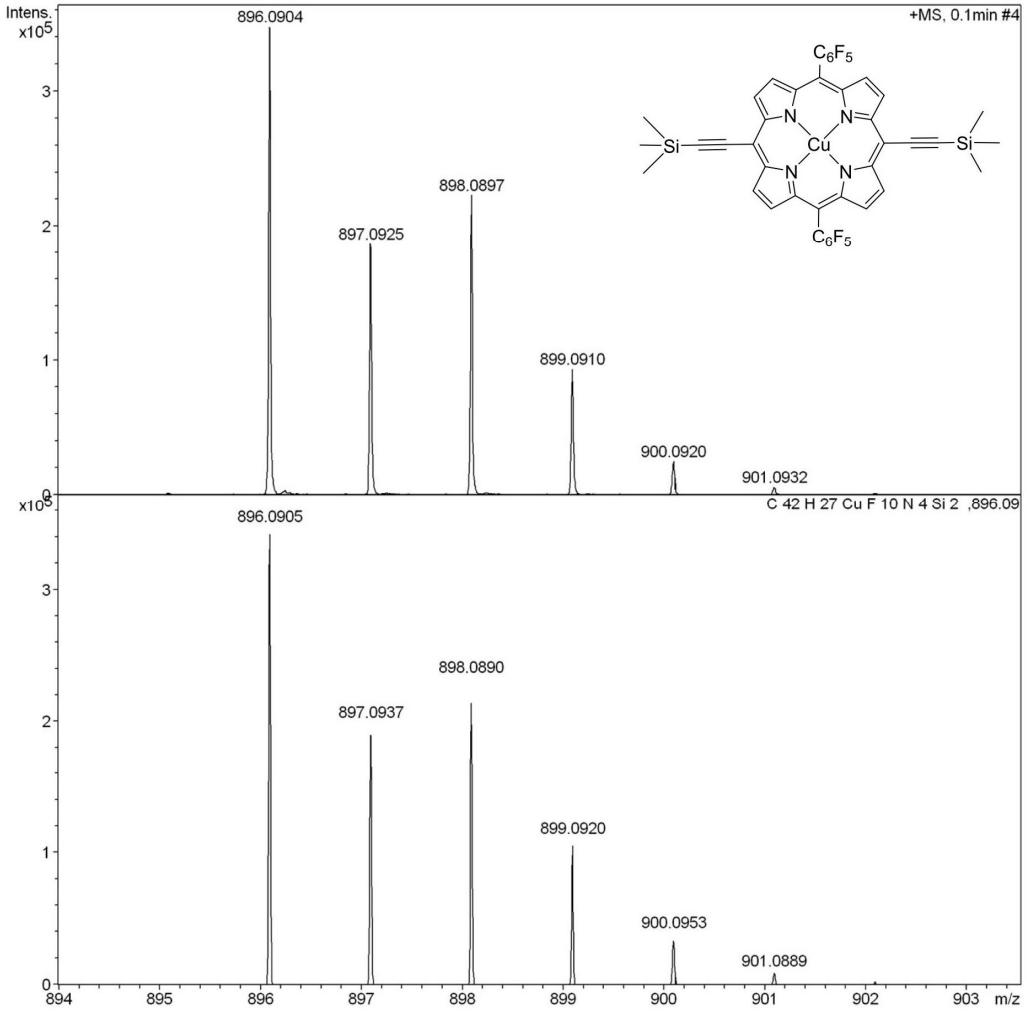

Fig. S4 HRMS of **c** in methanol. The ion at a mass-to-charge ratio of 896.0904 matches the calculated value of 896.0905 for the monocation of $[C_{42}H_{27}CuF_{10}N_4Si_2]^+$.

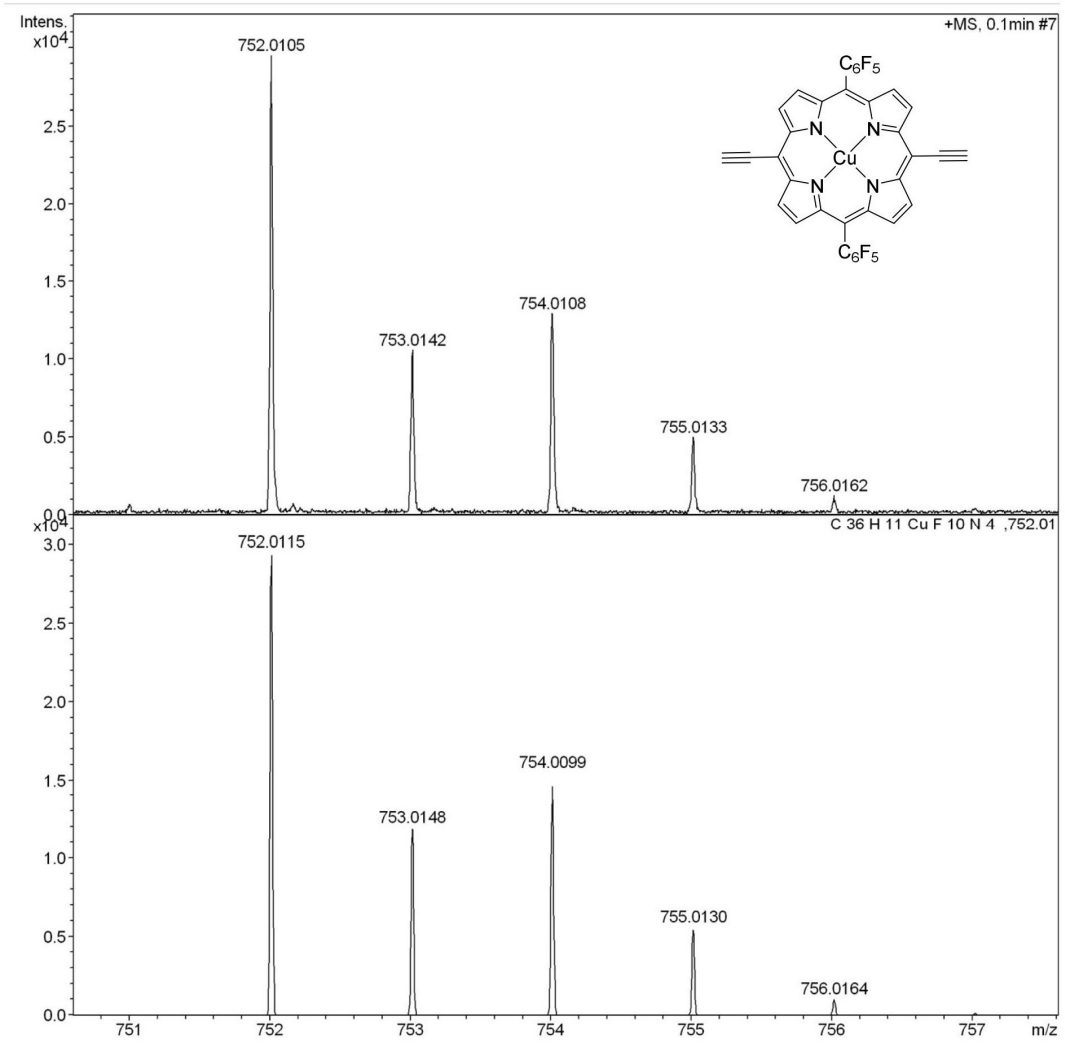

Fig. S5 HRMS of **d** in methanol. The ion at a mass-to-charge ratio of 752.0105 matches the calculated value of 752.0115 for the monocation of $[C_{36}H_{11}CuF_{10}N_4]^+$.

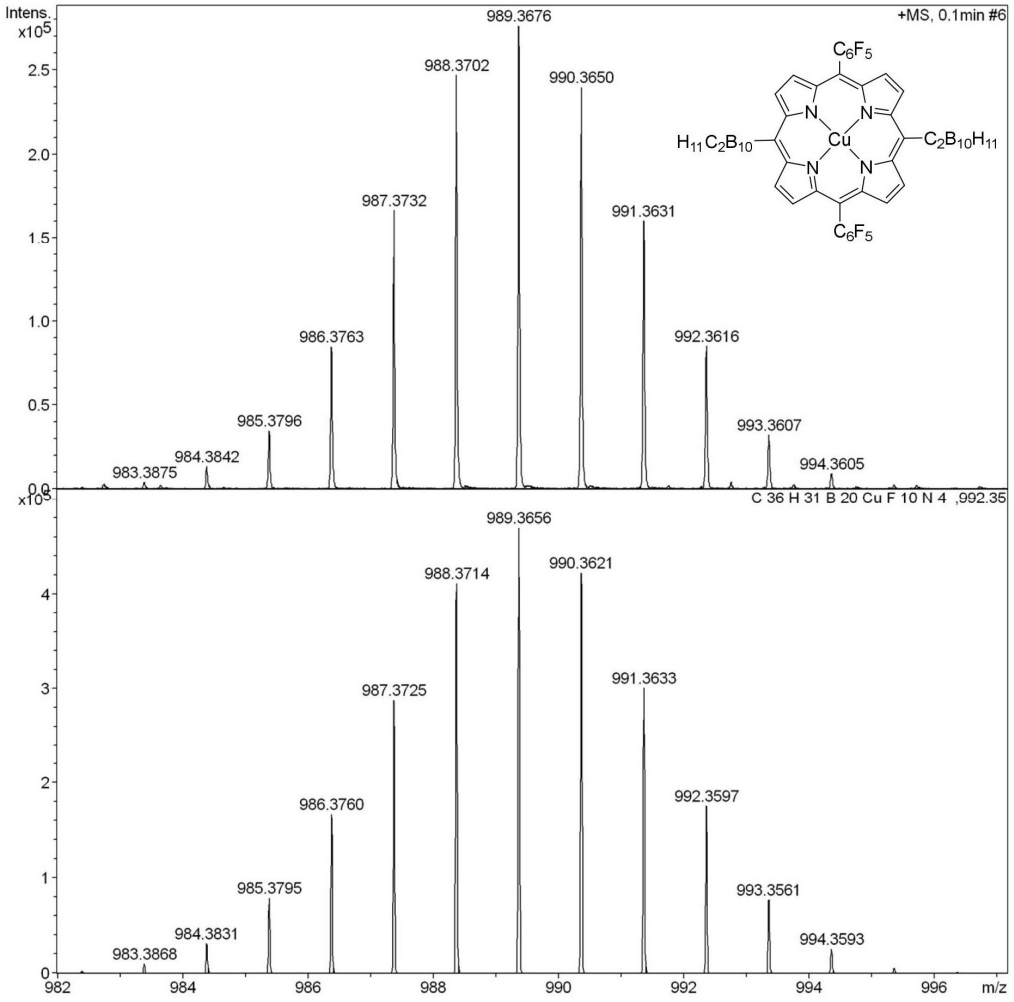

Fig. S6 HRMS of **1** in methanol. The ion at a mass-to-charge ratio of 992.3616 matches the calculated value of 992.3597 for the monocation of $[C_{36}H_{31}B_{20}CuF_{10}N_4]^+$.

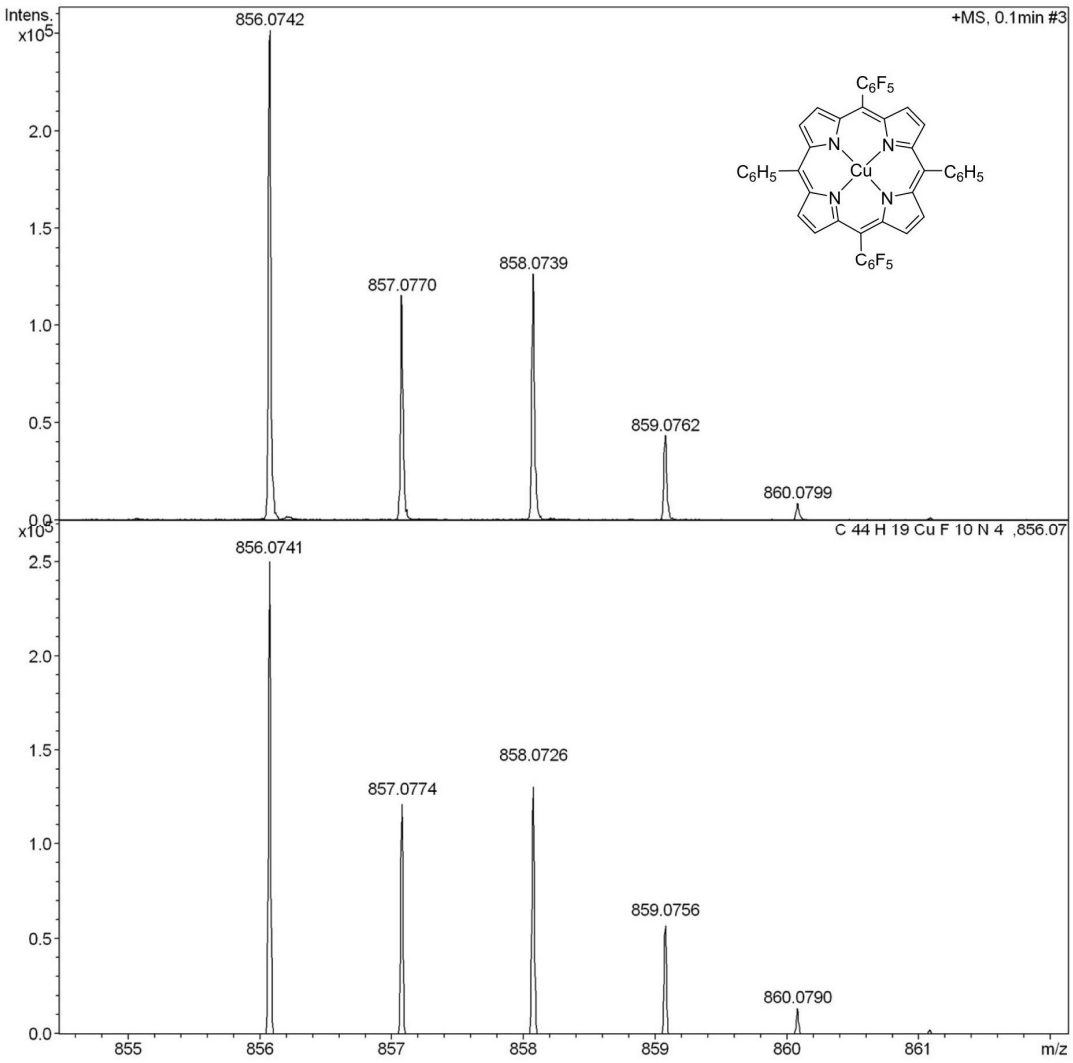

Fig. S7 HRMS of **2** in methanol. The ion at a mass-to-charge ratio of 856.0742 matches the calculated value of 856.0741 for the monocation of $[C_{44}H_{19}CuF_{10}N_4]^+$.

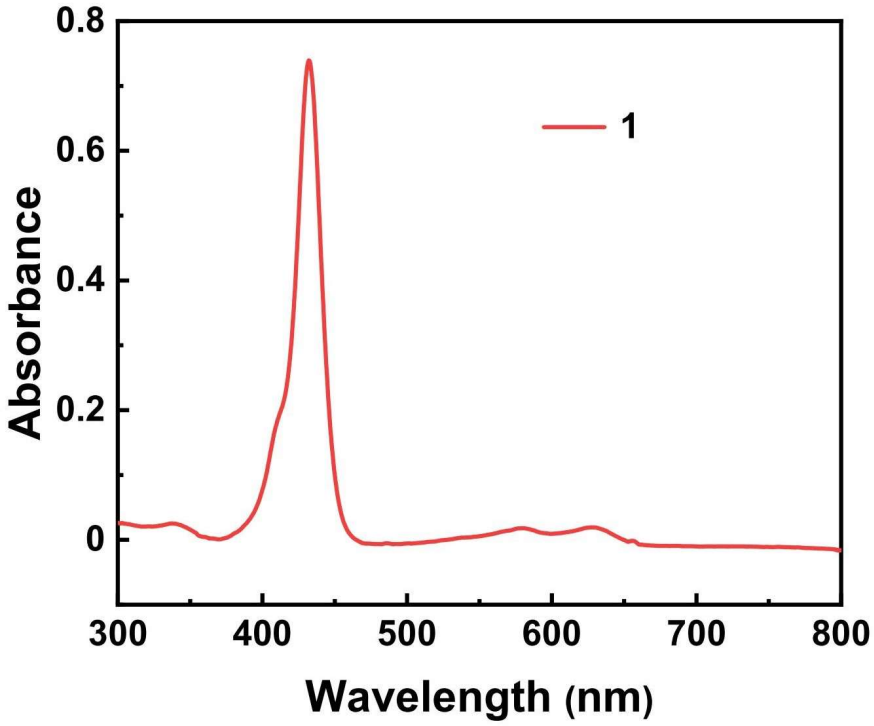

Fig. S8 UV-vis spectrum of **1** in acetonitrile.

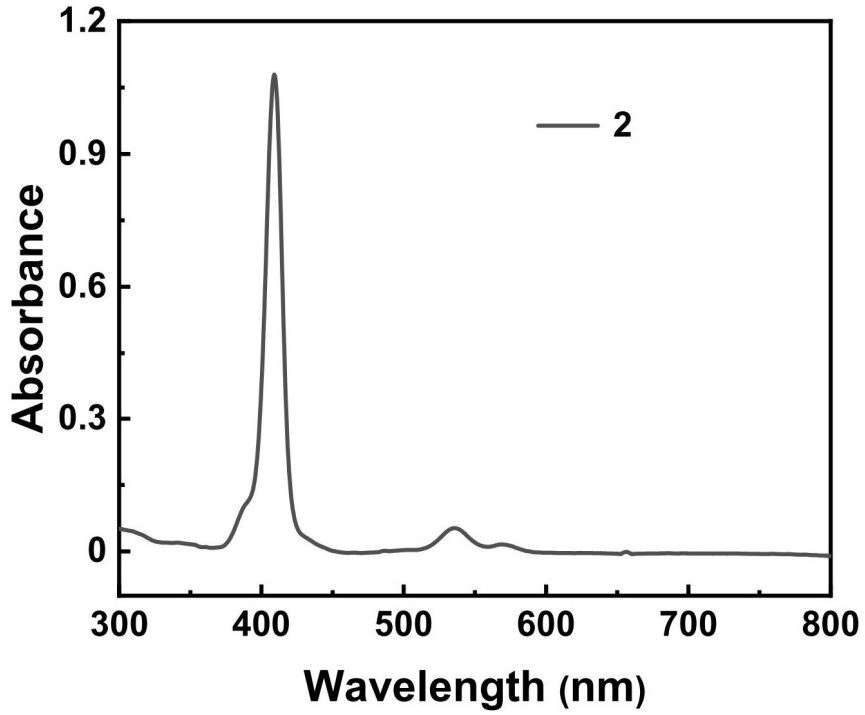

Fig. S9 UV-vis spectrum of **2** in acetonitrile.

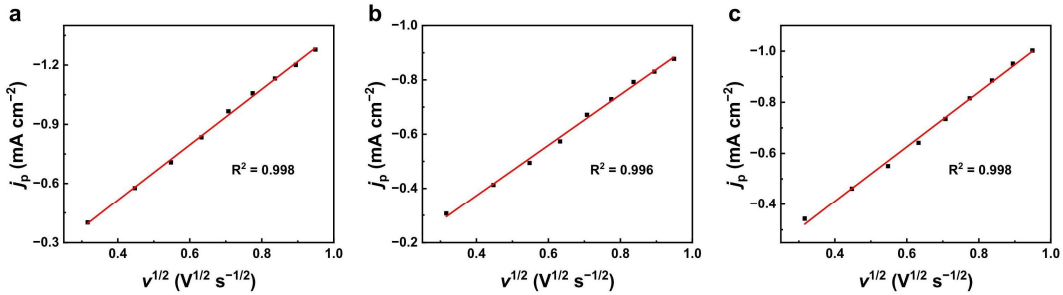

Fig. S10 The reduction peak currents of **1** at $E_{1/2}$ = −1.00 V (a), −1.64 V (b) and −1.80 V (c) versus the square root of scan rates. The potentials are referenced to ferrocene.

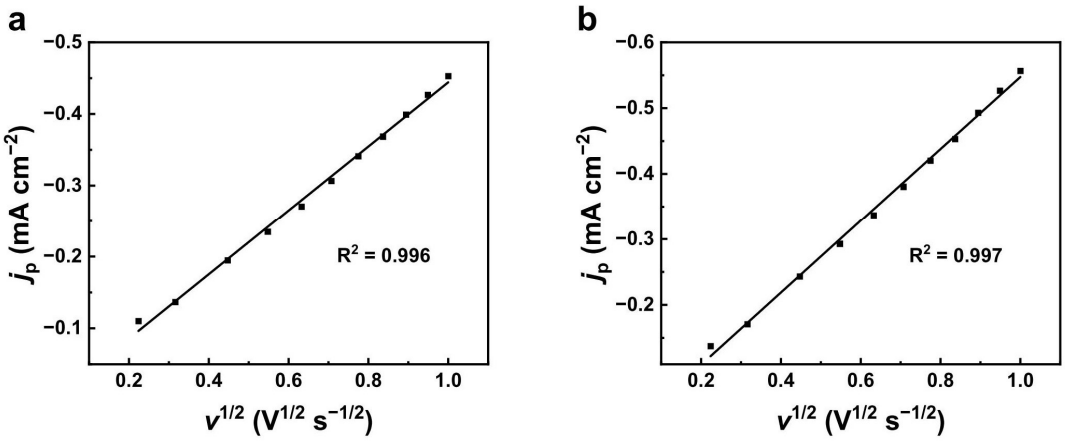

Fig. S11 The reduction peak currents of **2** at $E_{1/2}$ = −1.47 V (a) and −1.97 V (b) versus the square root of scan rates. The potentials are referenced to ferrocene.

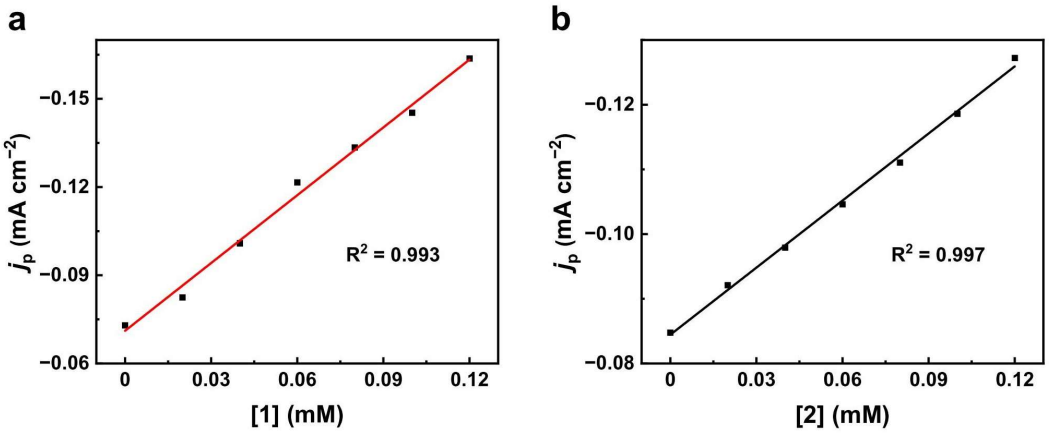

Fig. S12 Plots of catalytic peak currents of 0.5 mM TFA in acetonitrile with increasing **1** (a) and **2** (b), showing a first-order dependence.

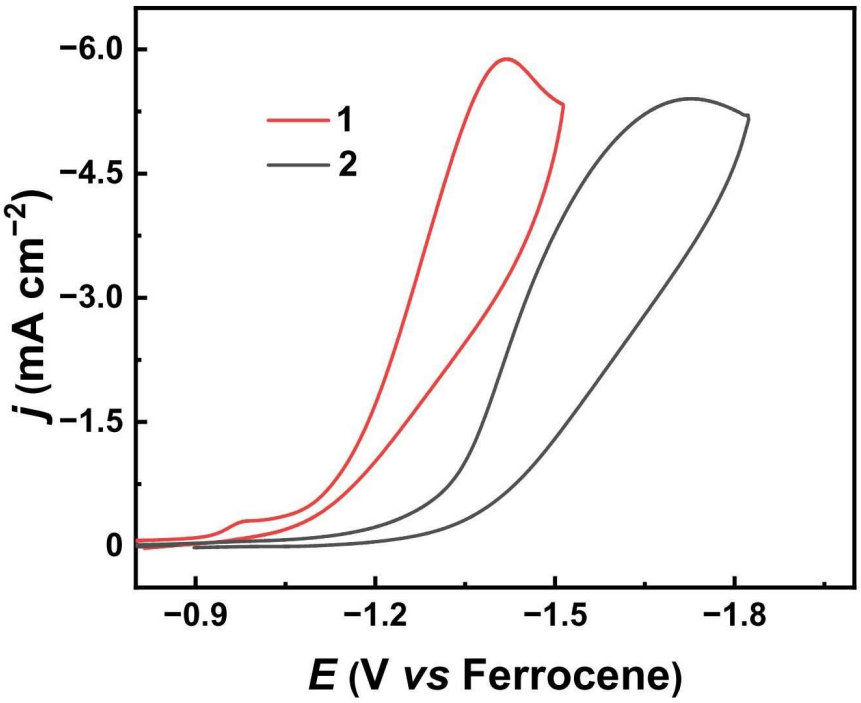

Fig. S13 CVs of **1** and **2** in acetonitrile with 100 equivalents of TFA.

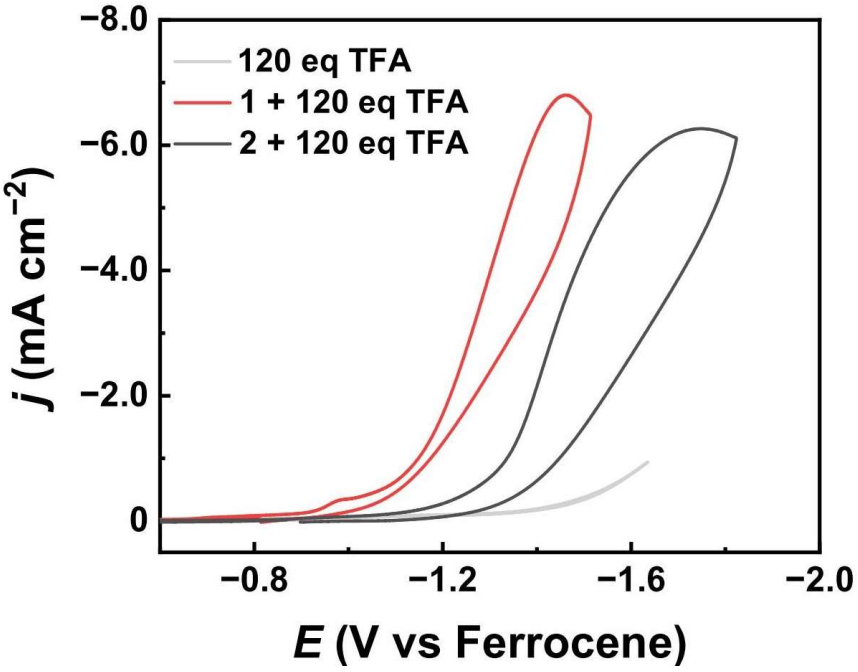

Fig. S14 CVs of TFA in acetonitrile containing **1**, **2**, and no catalyst.

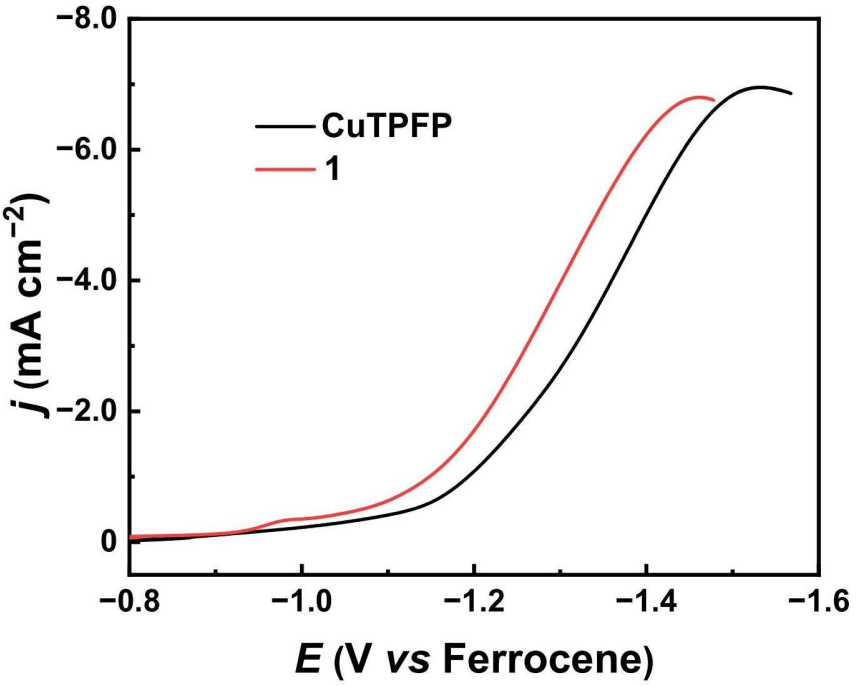

Fig. S15 LSVs of Cu porphyrin **1** and Cu tetrakis(pentafluorophenyl)porphyrin (CuTPFP) in acetonitrile with 120 equivalents of TFA.

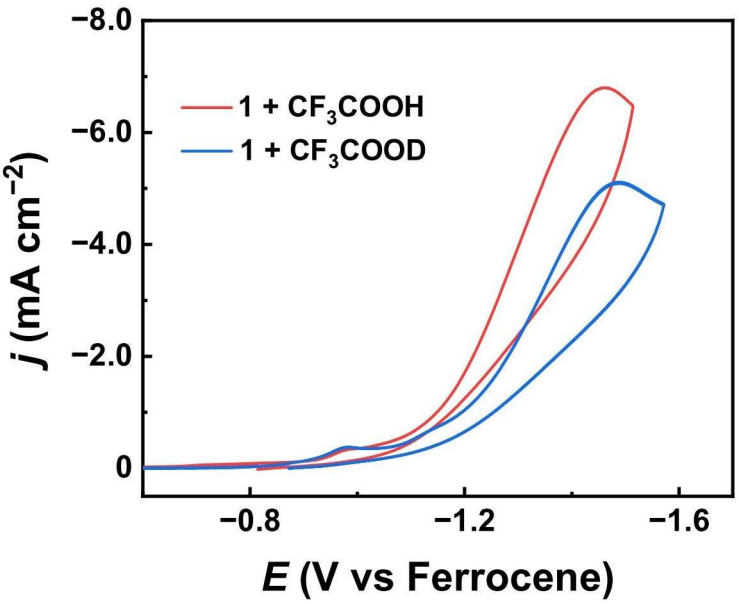

Fig. S16 CVs of **1** in acetonitrile with 120 equivalents of CF_3COOH and CF_3COOD.

The KIE value was calculated: $k_{cat,CF_3COOH}/k_{cat,CF_3COOD} = (i_{cat,CF_3COOH}/i_{cat,CF_3COOD})^2$.

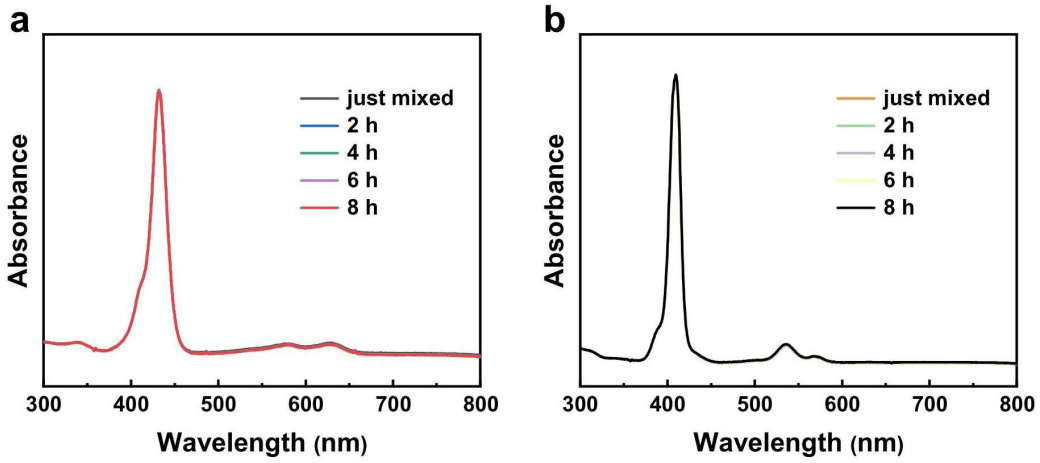

Fig. S17 UV-vis spectra of **1** (a) and **2** (b) in acetonitrile in the presence of 100 mM TFA, showing long-term acid durability.

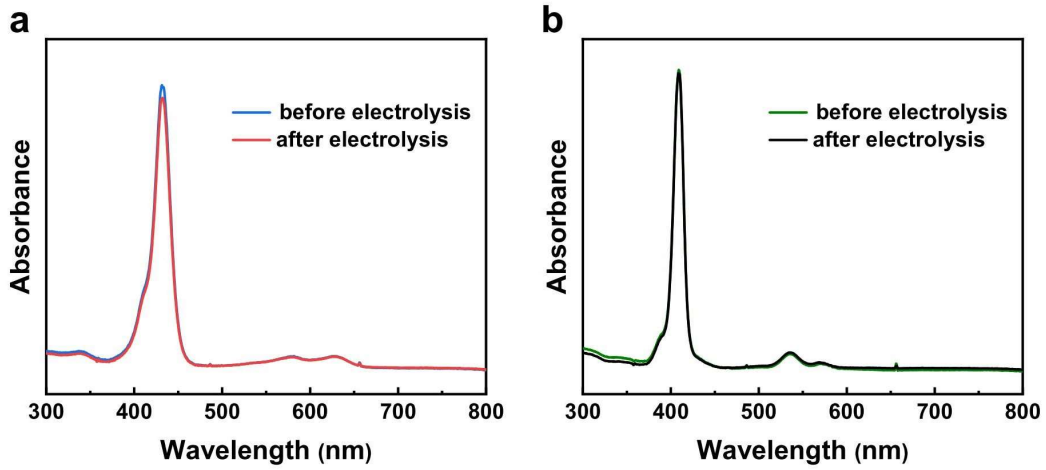

Fig. S18 UV-vis spectra of **1** (a) and **2** (b) in acetonitrile before and after electrolysis.

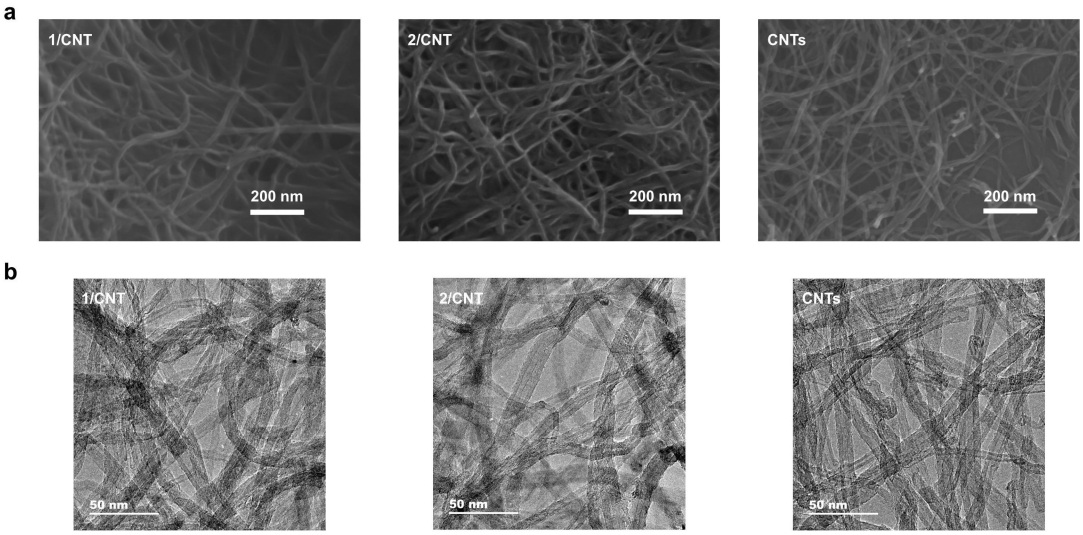

Fig. S19 SEM (a) and TEM (b) images of **1**/CNT, **2**/CNT, and CNTs.

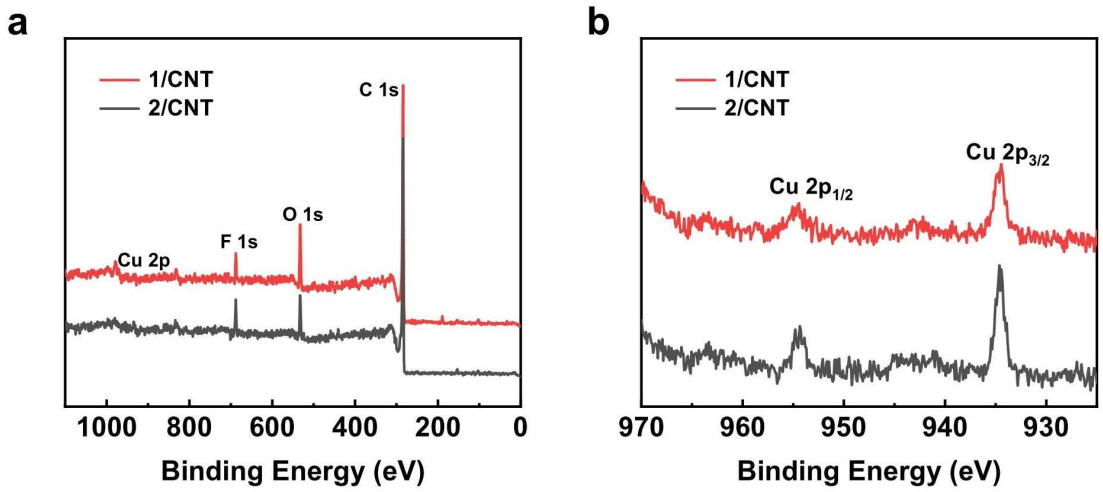

Fig. S20 XPS survey scan spectra of **1**/CNT and **2**/CNT (a) and the corresponding Cu 2p binding energy region (b).

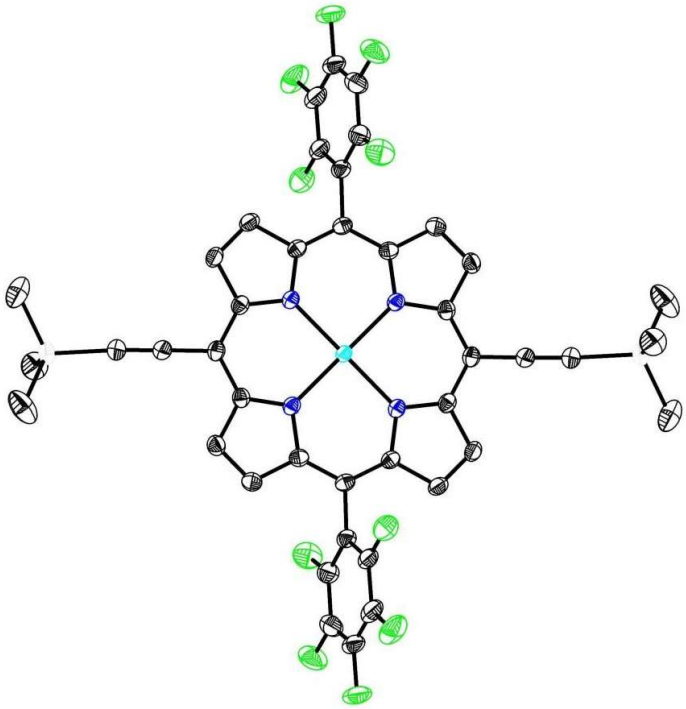

Fig. S21 Thermal ellipsoid plots (30% probability) of the X-ray structure of **c**. H atoms are omitted for clarity.

Table S1 Crystal data and structure refinement parameters for the X-ray structure of **1**, **2**, and **c**.

Complex	**1**	**2**	**c**
molecular formula	$C_{36}H_{30}B_{20}CuF_{10}N_4$	$C_{44}H_{18}CuF_{10}N_4$	$C_{42}H_{26}CuF_{10}N_4Si_2$
formula wt. (g mol^{-1})	988.38	856.16	896.40
temperature (K)	153(2)	153(2)	153(2)
radiation (λ, Å)	0.71073	0.71073	0.71073
crystal system	Triclinic	Monoclinic	Monoclinic
space group	$P\bar{1}$	$P2_1/c$	$I2/a$
a (Å)	16.848(4) A	15.085(4)	24.2143(18)
b (Å)	19.459(6) A	9.9686(17)	6.3478(6)
c (Å)	20.879(7) A	12.308(3)	29.627(2)
α(°)	91.445(12)	90	90
β (°)	106.278(12)	111.988(12)	108.824(8)
γ (°)	113.063(9)	90	90
volume ($Å^3$)	5974(3)	1716.2(7)	4310.3(6)
Z	4	2	4
ρ_{calcd} (g cm^{-3})	1.099	1.657	1.381
μ (mm^{-1})	0.424	0.733	0.646
F(000)	1972	858	1972
crystal size (mm^3)	0.10 × 0.10 × 0.05	0.50 × 0.10 × 0.10	0.40 × 0.20 × 0.05
theta range	1.874 to 26.195	2.509 to 26.372	3.291 to 26.398°
reflections collected	145630	41782	47315
independent reflections	23707 [R(int) = 0.0642	3501 [R(int) = 0.0341	4343 [R(int) = 0.0557
completeness	99.8 %	99.7 %	98.7 %
goodness-of-fit on F^2	1.008	1.107	1.111
final R indices	$R_1{}^a$ = 0.0497	$R_1{}^a$ = 0.0290	$R_1{}^a$ = 0.0410
[R > 2σ (I)]	$wR_2{}^b$ = 0.1353	$wR_2{}^b$ = 0.0729	$wR_2{}^b$ = 0.1206
R indices (all data)	$R_1{}^a$ = 0.0603 $wR_2{}^b$ = 0.1424	$R_1{}^a$ = 0.0306 $wR_2{}^b$ = 0.0738	$R_1{}^a$ = 0.0430 $wR_2{}^b$ = 0.1221
largest diff. peak and hole (e $Å^{-3}$)	0.648 and −0.552	0.314 and −0.439	0.497 and −0.462

$^aR_1 = \Sigma||F_o| - |F_c|| / |F_o|$, $^bwR_2 = \{\Sigma[w(F_o^2 - F_c^2)^2] / \Sigma[w(F_o^2)^2]\}^{0.5}$

Table S2 Electrocatalytic HER with **1** and reported metal porphyrins in acetonitrile.

Metal porphyrin	**[TFA]**	**Onset overpotential**	**Reference**
1	60.0 mM	300 mV	this work
SnPEGP	16.0 mM	480 mV	6
1-Co	50.0 mM	430 mV	7
Ni-2	60.0 mM	630 mV	8
Ga porphyrin 1	48.6 mM	430 mV	9
Ni porphyrin 3	4.00 mM	830 mV	10
Cu porphyrin 6	30.0 mM	480 mV	11
Ni complex 6	20.0 mM	630 mV	12

Table S3 Electrocatalytic HER with **1** and reported metal porphyrins and corroles in aqueous solutions.

Catalyst	**Medium**	**Overpotential at 50 mA cm^{-2}**	**Reference**
1	0.5 M H_2SO_4	852 mV	this work
[Co(tpfc)(py)$_2$]	0.5 M H_2SO_4	976 mV	13
CoTFPP	0.5 M H_2SO_4	> 900 mV	14
CoTPP	0.5 M H_2SO_4	> 900 mV	14
NiTAPP-Pyrene	0.5 M H_2SO_4	790 mV	15
Co corrole 1-Py	0.5 M H_2SO_4	830 mV	16
Co corrole 2-Py	0.5 M H_2SO_4	890 mV	16
CoPc Py-Py	0.5 M H_2SO_4	700 mV	17
CoPPh$_3$ corrole	0.5 M H_2SO_4	> 800 mV	18
Co(dmgBF$_2$)$_2$(MeCN)$_2$	phosphate-buffer pH 2	> 900 mV	19

Supporting References:

1 Y. Wang, X.-P. Zhang, H. Lei, K. Guo, G. Xu, L. Xie, X. Li, W. Zhang, U.-P. Apfel and R. Cao, *CCS Chem.*, 2022, **4**, 2959-2967.

2 *APEX v2009*, Bruker AXS, Madison, WI, 2009.

3 G. M. Sheldrick, *SADABS, 2008/1*, University of Göttingen, Göttingen, Germany, 2008.

4 G. M. Sheldrick, *Acta Crystallogr., Sect. A: Found. Crystallogr.*, 1990, **46**, 467-473.

5 G. M. Sheldrick, *Acta Crystallogr., Sect. A: Found. Crystallogr.*, 2008, **64**, 112-122.

6 A. Chaturvedi, G. A. McCarver, S. Sinha, E. G. Hix, K. D. Vogiatzis and J. Jiang, *Angew. Chem. Int. Ed.*, 2022, **61**, e202206325.

7 A. G. Maher, G. Passard, D. K. Dogutan, R. L. Halbach, B. L. Anderson, C. J. Gagliardi, M. Taniguchi, J. S. Lindsey and D. G. Nocera, *ACS Catal.*, 2017, **7**, 3597-3606.

8 Z.-Y. Wu, T. Wang, Y.-S. Meng, Y. Rao, B.-W. Wang, J. Zheng, S. Gao and J.-L. Zhang, *Chem. Sci.*, 2017, **8**, 5953-5961.

9 N. Wang, H. Lei, Z. Zhang, J. Li, W. Zhang and R. Cao, *Chem. Sci.*, 2019, **10**, 2308-2314.

10 X. Guo, N. Wang, X. Li, Z. Zhang, J. Zhao, W. Ren, S. Ding, G. Xu, J. Li, U.-P. Apfel, W. Zhang and R. Cao, *Angew. Chem. Int. Ed.*, 2020, **59**, 8941-8946.

11 Q. Zhang, H. Lei, H. Guo, Y. Wang, Y. Gao, W. Zhang and R. Cao, *ChemSusChem*, 2022, **15**, e202200086.

12 Z.-Y. Wu, H. Xue, T. Wang, Y. Guo, Y.-S. Meng, X. Li, J. Zheng, C. Brückner, G. Rao, R. D. Britt and J.-L. Zhang, *ACS Catal.*, 2020, **10**, 2177-2188.

13 H. Lei, A. Han, F. Li, M. Zhang, Y. Han, P. Du, W. Lai and R. Cao, *Phys. Chem. Chem. Phys.*, 2014, **16**, 1883-1893.

14 G. Xu, H. Lei, G. Zhou, C. Zhang, L. Xie, W. Zhang and R. Cao, *Chem. Commun.*, 2019, **55**, 12647-12650.

15 I. K. Attatsi, H. Zhong, J. Du, W. Zhu, M. Li and X. Liang, *Inorgnica Chimica Acta*, 2020, **503**, 119398.

16 X. Li, H. Lei, X. Guo, X. Zhao, S. Ding, X. Gao, W. Zhang and R. Cao, *ChemSusChem*, 2017, **10**, 4632-4641.

17 T. Gu, I. K. Attatsi, W. Zhu, M. Li, S. A. Ndur and X. Liang, *Inorgnica Chimica Acta*, 2022, **530**, 120696.

18 X. Liang, Y. Qiu, X. Zhang and W. Zhu, *Dalton Trans.*, 2020, **49**, 3326-3332.

19 L. A. Berben and J. C. Peters, *Chem. Commun.*, 2010, **46**, 398-400.